JACS
JOURNAL OF THE AMERICAN CHEMICAL SOCIETY
Communication
pubs.acs.org/JACS

Metal–Organic Frameworks as Micromotors with Tunable Engines and Brakes

Jinxing Li,[†] Xiao Yu,[†,‡] Mingli Xu,[†] Wenjuan Liu,[†] Elodie Sandraz,[†] Hsin Lan,[†] Joseph Wang,*[,†] and Seth M. Cohen*[,‡]

[†]Department of Nanoengineering, University of California, San Diego, La Jolla, California 92093, United States
[‡]Department of Chemistry and Biochemistry, University of California, San Diego, La Jolla, California 92093, United States

Supporting Information

ABSTRACT: Herein, we report that UiO-type (UiO = University of Oslo) metal–organic frameworks (MOFs) can be transformed into self-propelled micromotors by employing several different metal-based propulsion systems. Incorporation of a bipyridine ligand into the UiO-67 lattice transforms the crystallites, upon metalation, into single-site, metal-based catalytic "engines" to power the micromotors with chemical fuel. The "engine performance" (i.e., propulsion) of the single-site powered micromotors has been tuned by the choice of the metal ion utilized. In addition, a chemical "braking" system was achieved by adding chelating agents capable of sequestering the metal ion engines and thereby suppressing the catalytic activity, with different chelators displaying different deceleration capacities. These results demonstrate that MOFs can be powered by various engines and halted by different brakes, resulting in a high degree of motion design and control at the nanoscale.

The complex transport processes in living cells are possible because of a set of highly efficient and functional biomolecular motors. Recently, there has been a strong interest in the development of organic and inorganic devices and machines that are capable of efficient propulsion and complex operation at the nanoscale through energy consumption.[1−8] Among the many micro/nanoscale machines, bubble-propelled micromotors are quite powerful and versatile for many practical operations such as biological target transportation and isolation,[9] drug delivery,[10−12] and environmental remediation.[13−15] Bubble propulsion commonly involves catalytic decomposition of hydrogen peroxide as a fuel using a catalytic engine to generate oxygen bubbles.[16] Inorganic catalysts including the noble metals Pt and Ag, as well as enzyme catalysts such as catalase, have been used for catalytic propulsion.[17−19] However, the most widely used catalyst, based on Pt metal, is expensive and enzymatic systems such as catalase have limited stability. In most of these systems, the speeds of the bubble propulsion motors are controlled by the amount of fuel used and are difficult to be tuned or halted at will. Given these limitations, there is a strong desire to develop low cost, tunable micromotors with different engines and functional materials for various on-demand operations.

Metal–organic frameworks (MOFs) have emerged as a class of microporous crystalline materials with high surface areas and tunable pore microenvironments that can be applied to challenges in gas storage/separation, chemical sensing, catalysis, and drug delivery.[20,21] Both presynthetic and postsynthetic methods have been widely investigated to obtain functionalized MOFs.[22] Importantly, MOFs with accessible metal-binding sites can be readily prepared to provide site-isolated catalytic sites.[23,24]

The use of MOFs to build micro/nanomachines has received little attention, despite the tremendous chemical diversity and tunability of these coordination solids. To the best of our knowledge, only a few reports on MOF-based motor devices have been described.[25−27] Two reports used the Marangoni effect generated by peptide-driven self-assembly as the locomotive source to drive millimeter-size MOF particle.[25,26] A third report used ZIF-67/ZIF-8 Janus particles, with sizes between 200 and 500 μm, that were propelled via the catalytic decomposition of H_2O_2 by the Co^{2+}-based ZIF-67 part of the particle.[27] Although these pioneering reports are at the interface of MOFs and tiny motors, they utilize strategies that have limitations with respect to the choice of MOF that can be used, the types of the motors that can be achieved, and the degree of control over propulsion.

Herein, we report facile preparation of micromotors from the widely used Zr^{4+}-based UiO-67 MOF scaffold. The Zr^{4+}-based UiO (UiO = University of Oslo) series of MOFs were selected due to their high chemical stability and tunability.[28] UiO-based micromotors were generated by introducing single-site metal centers on the ligand struts that catalyze the decomposition of H_2O_2 fuel (Figure 1). This approach offers a very facile and diverse means of manufacturing MOF micromotors. Most importantly, the catalytic activity of the "engine" can be tuned by the choice of metal ion utilized. In addition, adding suitable chelators as "brakes" could reduce the micromotor speed, further demonstrating the high degree of control and tunability in this MOF micromotor system.

A mixed-ligand method was used to synthesize UiO-67-$bpy_{0.25}$ MOF as the platform, where 25% H_2dcbpy (2,2′-bipyridine-dicarboxylic acid) was mixed with H_2bpdc (biphenyldicarboxylic acid) as connecting ligands (Figure 1a). During the synthesis, a large excess of benzoic acid was added as a modulator, producing monodisperse particles ∼5 μm in diameter. Metalation of the bipyridine sites with cobalt or

Received: November 17, 2016
Published: December 19, 2016

DOI: 10.1021/jacs.6b11899
J. Am. Chem. Soc. 2017, 139, 611−614

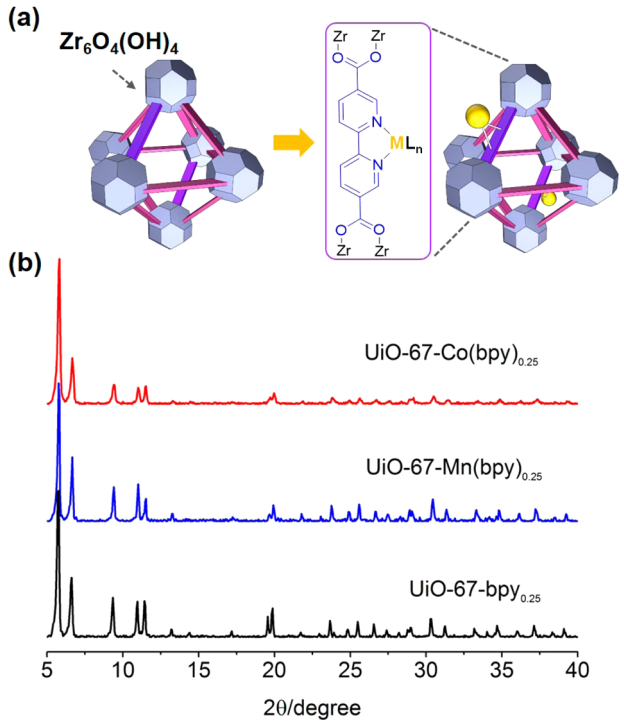

Figure 1. Zr-based MOF micromotors. (a) Scheme of the metalation of UiO-67-bpy$_{0.25}$, (b) PXRD of UiO-67-bpy$_{0.25}$, UiO-67-Mn(bpy)$_{0.25}$, and UiO-67-Co(bpy)$_{0.25}$ MOFs.

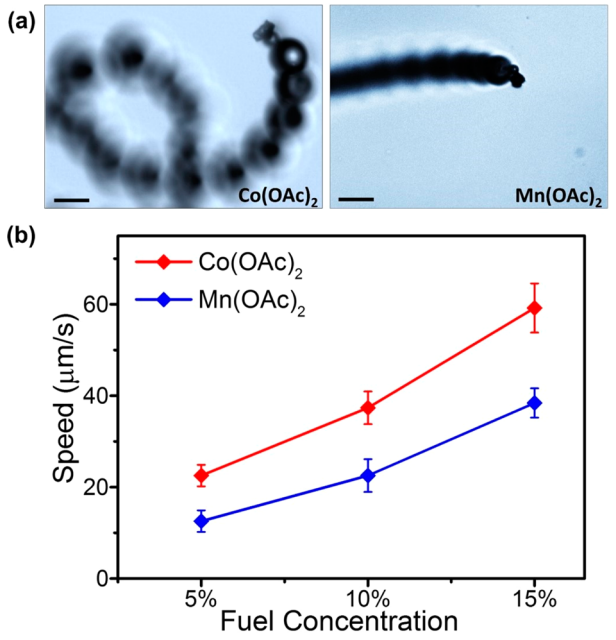

Figure 2. Tuning the speed of micromotor engines with different metals. (a) Microscopy images showing the propulsion of micromotor engines made from UiO-67-bpy$_{0.25}$ metalated with Co^{2+} and Mn^{2+}. Scale bars: 10 μm. (b) Speed of the different MOF micromotor engines as a function of fuel concentration. Plots are based on measuring the average speed of 30 tracked MOF particles.

manganese salts afforded single-site catalytically active MOF nanomotors with good crystallinity, which was confirmed by powder X-ray diffraction (Figure 1b). SEM with EDX (energy dispersive X-ray spectroscopy) was used to characterize the metal ratio of metalated UiO-67 (Figure S1, Table S1). For Co^{2+}-metalated UiO-67-bpy$_{0.25}$, using Co(OAc)$_2$ (OAc = acetate) as the metal source, postsynthetic modification (PSM) yielded 20% overall metalation, which is equivalent to metalation of 80% of the available bipyridine sites in the MOF. For Mn^{2+}-metalated UiO-67-bpy$_{0.25}$, Mn(OAc)$_2$ was found to modify quantitatively UiO-67-bpy$_{0.25}$. EDX mapping (Figure S1) showed the uniform distribution of Co^{2+} and Mn^{2+} in these MOFs.

The resulting UiO-67-Co(bpy)$_{0.25}$ and UiO-67-Mn(bpy)$_{0.25}$ can work as micromotors in fuel solutions, where the metal-based catalytic engine sites decompose H_2O_2 into water and oxygen for bubble-propelled motion (Figure 2, Supporting Video 1). Control experiments were conducted to confirm the role of the catalytic active sites in these MOF motors. A nonmetalated UiO-67-bpy$_{0.25}$ crystal showed no motion in a 5% (v/v) H_2O_2 aqueous solution (no bubbling, Supporting Video 2). Similarly, as-synthesized UiO-67 without any bipyridine sites (only H_2bpdc as a ligand), even when treated with Co(OAc)$_2$, did not move in H_2O_2 fuel solutions. The metalated MOF micromotors show efficient motion for at least 6 h with a continuous supply of fuel. These control experiments indicate that the binding of suitable metal ions at the MOF bipyridine sites is essential to form the catalytic engine.

As expected, when evaluated at different fuel levels (5%, 10%, 15% (v/v) H_2O_2), higher concentrations of H_2O_2 fuel solution gave rise to faster movement of both UiO-67-Co(bpy)$_{0.25}$ and UiO-67-Mn(bpy)$_{0.25}$ particles (Figure 2a). These data show a rapid conversion of chemical energy into mechanical work with increasing fuel concentration. Importantly, greater speeds were observed at all fuel concentrations with UiO-67-Co(bpy)$_{0.25}$ when compared to UiO-67-Mn(bpy)$_{0.25}$ (Figure 2b), despite the manganese system having a higher loading of metal ion. This shows that by selecting different metal ions we can tune the performance of the engines in these MOF micromotors. It is observed that the moving direction of the MOF micromotors is random due to the inhomogeneous bubble nucleation on the crystal surface. However, coating with a magnetic layer, such as Ni or Fe, could enable remote magnetic guidance of the MOF motors.[17,29−33]

Interestingly, the propulsion of UiO-67 micromotors can be dramatically slowed down and stopped by adding suitable chelators as chemical brakes. This can be achieved by adding chelating ligands such as iminodiacetic acid (IDA) or ethylenediaminetetraacetic acid (EDTA) into the motor-fuel system. The attenuated motion of the MOF motors in the presence of chelator brakes was clearly indicated by a reduction in the ejection of oxygen bubbles from the crystal. Figure 3 displays time-lapse images (taken from Supporting Video 3) illustrating changes in the motion of the UiO-67-Co(bpy)$_{0.25}$ motor in the presence of IDA with a fuel concentration of 15% (v/v) H_2O_2. The track lines in Figure 3a were recorded over a 2 s period following 0 and 15 min exposures to IDA. A clear reduction in bubble ejection and propulsion is observed after adding IDA, with movement of the MOF effectively halted.

A comparative study of the braking behaviors of UiO-67-Co(bpy)$_{0.25}$ and UiO-67-Mn(bpy)$_{0.25}$ micromotors in the presence of IDA or EDTA is shown in Figure 3, in which the normalized speed of motors is tracked over a 30 min period. In the absence of chemical brakes, both motors only show slightly decreases in speed over a 30 min period (due to the depletion of fuel). However, the addition of IDA or EDTA resulted in steep drops in speed, even after only 5 min, and completely braking is observed at ∼20 min (EDTA) and ∼30 min (IDA).

DOI: 10.1021/jacs.6b11899
J. Am. Chem. Soc. 2017, 139, 611−614

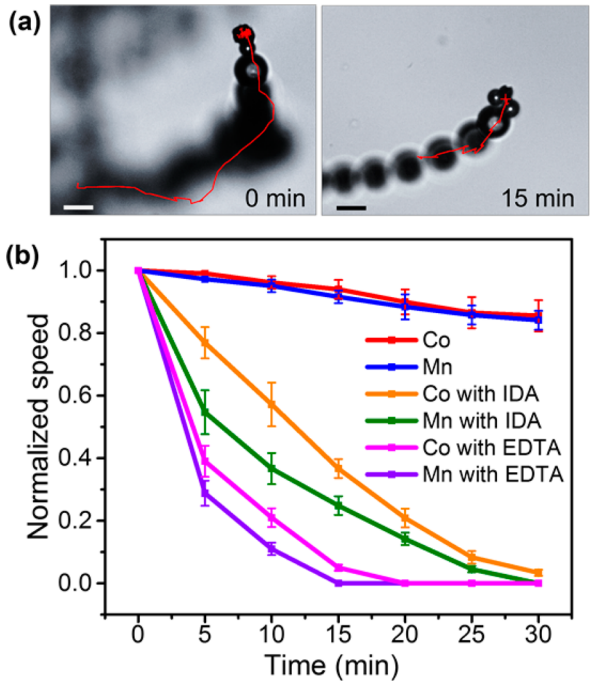

Figure 3. Chelators act as molecular brakes for MOF micromotors. (a) Microscopy images showing the propulsion of UiO-67-Co(bpy)$_{0.25}$ at the 0 and 15 min after adding IDA (0.15 M). The red trajectories indicate the motion in 2 s. Scale bars: 10 μm. (b) Time-dependent normalized speed of the micromotor engines UiO-67-Co(bpy)$_{0.25}$ and UiO-67-Mn(bpy)$_{0.25}$ before and after adding chemical brakes: either 0.15 M IDA or EDTA. Fuel concentration: 15% (v/v) H_2O_2.

The motor tracking data of Figure 3b clearly illustrate that EDTA is a more effective brake, which is consistent with the greater chelating ability of EDTA versus IDA.[32] Similarly, UiO-67-Mn(bpy)$_{0.25}$ motors proved to be more susceptible to the chemical brakes than UiO-67-Co(bpy)$_{0.25}$ (Figure 3b), which is consistent with lower stability of the Mn(bpy) when compared to Co(bpy) complex.[33]

To investigate the mechanism of braking, the metal content of the MOF motors after exposure to either IDA or EDTA was measured by EDX. The EDX data show (Table S1) that ~95% of the Co and Mn were removed from the MOF motors after 30 min exposure to the chemical brakes. The decrease in content upon braking is consistent with a mechanism involving removal engine metals from the active sites of the MOF motors, resulting in the loss of propulsion. To ensure that braking is not due to these chelators destroying the MOF, PXRD, and SEM was used to show that these MOFs maintain crystallinity after 30 min incubation in 0.15 M IDA or EDTA solution (Figure S2, S3). In addition, the MOF micromotors showed no change in bulk structure, as gauged by microscopic imaging, over the course of the experiment (30 min).

In conclusion, single-site catalytic MOFs can act as self-propelled micromotors. The propulsion of MOF-nanomotors can be tuned by the metal ion used to power the micromotor engine. In addition, a braking system has been achieved by adding chelator brakes to remove the catalytic engine metal ions, thus controlling the speed and motion of micromotors. We expect that the strategy employed here for micromotors is adaptable to a much wider variety of MOFs when compared to previously reported approaches. Integrating the functionality of MOF materials with self-propelled micro/nanomachines will significantly advance the implementation of active transport in catalysis, energy storage and conversion, environmental decontamination, and other applications.

■ ASSOCIATED CONTENT

Supporting Information

The Supporting Information is available free of charge on the ACS Publications website at DOI: 10.1021/jacs.6b11899.

Experimental details, additional characterization of MOF catalysts and catalysis reactions (PDF)

Propulsion of UiO-67-bpy$_{0.25}$ micromotor engines metalated with Co^{2+} and Mn^{2+} in a peroxide fuel concentration of 15% (AVI)

Behavior of UiO-67-bpy$_{0.25}$ crystal without metalation compared with the same micromotor metalated with Co^{2+} in a peroxide fuel concentration of 5% (AVI)

Propulsion of UiO-67-Co(bpy)$_{0.25}$ micromotor engine (metallated with Co^{2+}) at the 0 min and 15 min after adding IDA (0.15 M) braking (AVI)

■ AUTHOR INFORMATION

Corresponding Authors

*S.M.C. scohen@ucsd.edu

*J.W. josephwang@eng.ucsd.edu

ORCID

Seth M. Cohen: 0000-0002-5233-2280

Author Contributions

J.L. and X.Y. contributed equally.

Notes

The authors declare no competing financial interest.

■ ACKNOWLEDGMENTS

This work was supported by grants from the National Science Foundation, Division of Chemistry (CHE-1359906 to S.M.C.) and the Defense Threat Reduction Agency Joint Science and Technology Office for Chemical and Biological Defense (Grant Nos. HDTRA1-14-1-0064 to J.W.). M.X. and W.L. acknowledge the China Scholarship Council (CSC) for the financial support.

■ REFERENCES

(1) Balzani, V.; Credi, A.; Raymo, F. M.; Stoddart, J. F. *Angew. Chem., Int. Ed.* **2000**, *39*, 3348.

(2) Browne, W. R.; Feringa, B. L. *Nat. Nanotechnol.* **2006**, *1*, 25.

(3) Wang, J. *Nanomachines: Fundamentals and Applications*; John Wiley & Sons, 2013.

(4) Sanchez, S.; Soler, L.; Katuri, J. *Angew. Chem., Int. Ed.* **2015**, *54*, 1414.

(5) Wang, W.; Duan, W.; Ahmed, S.; Mallouk, T. E.; Sen, A. *Nano Today* **2013**, *8*, 531.

(6) Mei, Y.; Solovev, A. A.; Sanchez, S.; Schmidt, O. G. *Chem. Soc. Rev.* **2011**, *40*, 2109.

(7) Wang, H.; Pumera, M. *Chem. Rev.* **2015**, *115*, 8704.

(8) Guix, M.; Mayorga-Martinez, C. C.; Merkoçi, A. *Chem. Rev.* **2014**, *114*, 6285.

(9) Balasubramanian, S.; Kagan, D.; Hu, C.-M.; Campuzano, S.; Lobo-Castañon, M. J.; Lim, N.; Kang, D. Y.; Zimmerman, M.; Zhang, L.; Wang, J. *Angew. Chem., Int. Ed.* **2011**, *50*, 4161.

(10) Mou, F.; Chen, C.; Zhong, Q.; Yin, Y.; Ma, H.; Guan, J. *ACS Appl. Mater. Interfaces* **2014**, *6*, 9897.

(11) Wu, Z.; Wu, Y.; He, W.; Lin, X.; Sun, J.; He, Q. *Angew. Chem., Int. Ed.* **2013**, *52*, 7000.

DOI: 10.1021/jacs.6b11899
J. Am. Chem. Soc. 2017, 139, 611−614

(12) Li, J.; Thamphiwatana, S.; Liu, W.; Esteban-Fernández de Ávila, B.; Angsantikul, P.; Sandraz, E.; Wang, J.; Xu, T.; Soto, F.; Ramez, V.; et al. *ACS Nano* **2016**, *10*, 9536.
(13) Orozco, J.; Cheng, G.; Vilela, D.; Sattayasamitsathit, S.; Vazquez-Duhalt, R.; Valdés-Ramírez, G.; Pak, O. S.; Escarpa, A.; Kan, C.; Wang, J. *Angew. Chem., Int. Ed.* **2013**, *52*, 13276.
(14) Soler, L.; Magdanz, V.; Fomin, V. M.; Sanchez, S.; Schmidt, O. G. *ACS Nano* **2013**, *7*, 9611.
(15) Srivastava, S. K.; Guix, M.; Schmidt, O. G. *Nano Lett.* **2016**, *16*, 817.
(16) Li, J.; Rozen, I.; Wang, J. *ACS Nano* **2016**, *10*, 5619.
(17) Solovev, A. A.; Mei, Y.; Bermúdez Ureña, E.; Huang, G.; Schmidt, O. G. *Small* **2009**, *5*, 1688.
(18) Wang, H.; Zhao, G.; Pumera, M. *J. Am. Chem. Soc.* **2014**, *136*, 2719.
(19) Sanchez, S.; Solovev, A. A.; Mei, Y.; Schmidt, O. G. *J. Am. Chem. Soc.* **2010**, *132*, 13144.
(20) Furukawa, H.; Cordova, K. E.; O'Keeffe, M.; Yaghi, O. M. *Science* **2013**, *341*, 1230444.
(21) Kitagawa, S.; Zhou, H.-C. *Chem. Soc. Rev.* **2014**, *43*, 5415.
(22) Cohen, S. M. *Chem. Rev.* **2012**, *112*, 970.
(23) Cohen, S. M.; Zhang, Z.; Boissonnault, J. A. *Inorg. Chem.* **2016**, *55*, 7281.
(24) Yu, X.; Cohen, S. M. *J. Am. Chem. Soc.* **2016**, *138*, 12320.
(25) Ikezoe, Y.; Washino, G.; Uemura, T.; Kitagawa, S.; Matsui, H. *Nat. Mater.* **2012**, *11*, 1081.
(26) Ikezoe, Y.; Fang, J.; Wasik, T. L.; Shi, M.; Uemura, T.; Kitagawa, S.; Matsui, H. *Nano Lett.* **2015**, *15*, 4019.
(27) Tan, T. T.; Cham, J. T.; Reithofer, M. R.; Hor, T. S.; Chin, J. M. *Chem. Commun.* **2014**, *50*, 15175.
(28) Kim, M.; Cohen, S. M. *CrystEngComm* **2012**, *14*, 4096.
(29) Gao, W.; Uygun, A.; Wang, J. *J. Am. Chem. Soc.* **2012**, *134*, 897.
(30) Gao, W.; Feng, X.; Pei, A.; Gu, Y.; Li, J.; Wang, J. *Nanoscale* **2013**, *5*, 4696.
(31) Li, J.; Gao, W.; Dong, R.; Pei, A.; Sattayasamitsathit, S.; Wang, J. *Nat. Commun.* **2014**, *5*, 5026.
(32) Smith, R. M.; Martell, A. E.; Motekaitis, R. *NIST critically selected stability constants of metal complexes database*; National Institute of Standards & Technology, 1998.
(33) Irving, H.; Mellor, D. *J. Chem. Soc.* **1962**, *0*, 5222.

DOI: 10.1021/jacs.6b11899
J. Am. Chem. Soc. 2017, 139, 611−614